# Muon Imaging Applications for Nuclear Waste Management and Decommissioning

**Anthony Clarkson,[1,2] Simon Gardner,[1,2] David Ireland,[1] Ramsey Jebali,[1] Ralf Kaiser,[1,2] David Mahon,[1,2] Matthew Ryan,[3] Craig Shearer,[3] and Guangliang Yang[1,2]**

[1]*School of Physics & Astronomy, University of Glasgow, University Avenue, Glasgow G12 8QQ, UK*
[2]*Lynkeos Technology Ltd., No 11 The Square, Glasgow G12 8QQ, UK*
[3]*National Nuclear Laboratory, Central Laboratory, Sellafield, Seascale, Cumbria CA20 1PG, UK*

*Corresponding author: Matthew Ryan*
*Email address: matt.j.ryan@uknnl.com*

## Abstract

In the UK nuclear industry, muon imaging is gaining traction as a credible option in the toolkit of techniques for monitoring and inspection of waste packages arising from decommissioning activities across the UK nuclear estate. Since 2009, the UK National Nuclear Laboratory has collaborated with the University of Glasgow and Lynkeos Technology Ltd. to develop muon imaging techniques for such applications. In this paper, we review our experiences in imaging typical waste forms such as vitrified products and corroded sludge. The requirements and expectations of stakeholders and plant operators with regard to waste monitoring are examined, and the constraints and challenges of deploying and operating muon detection instruments on nuclear-licensed sites are discussed.

*Keywords:* muography, nuclear waste, characterization, monitoring
*DOI:* 10.31526/JAIS.2022.256

## 1. INTRODUCTION

Sellafield in the UK is one of the largest nuclear sites in Europe. Since the 1940s, it has played host to various research facilities and spent fuel reprocessing plants which are now being decommissioned. These decommissioning activities often require processing and management of legacy wastes, which need to be characterized and monitored to satisfy safety cases and regulatory requirements.

Since 2009, a collaboration between the UK National Nuclear Laboratory (NNL), the University of Glasgow, and its spin-out company, Lynkeos Technology Ltd., has been developing muon imaging techniques to meet the challenges and requirements of nuclear site decommissioning and waste characterization and monitoring.

In this paper we briefly describe the Lynkeos Muon Imaging System (MIS), followed by a discussion of our experiences in imaging various waste packages and the challenges encountered in deploying muon detection equipment on a nuclear-licensed site.

## 2. MUON IMAGING SYSTEM

The Lynkeos MIS [1], shown in Figure 1, comprises two tracking modules above the imaging volume and two below to allow reconstruction of the incoming and outgoing (scattered) muon tracks. Each module has 1024 scintillating fibers (Saint-Gobain BCF-12, 2 mm diameter) in the $x$ direction and 1024 fibers in the $y$ direction arranged in a staggered, overlapping geometry. This configuration allows the determination of the muon hit position with mm precision.

The fibers are coupled to a pixel on a 64-channel Hamamatsu H12700A multi-anode photomultiplier tube (MAPMT) with two fibers per pixel to reduce the number of required read out channels (the demultiplexing of the two signals is performed in the track reconstruction software). The MAPMTs are read out by MAROC3A chips, integrated into an FPGA-controlled readout system designed by INFN Genoa.

Two such systems are currently operational: one at the University of Glasgow and one at the NNL Central Laboratory at Sellafield. The available imaging area of the system is approximately 1066 mm × 1066 mm and an aluminium support table allows imaging of objects up to 1 t in weight.

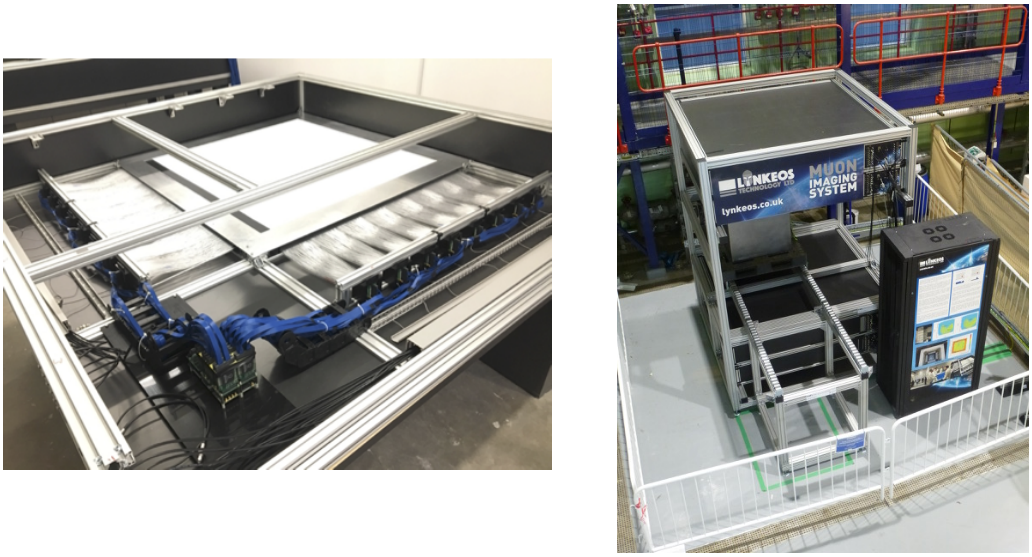

FIGURE 1: The interior of a tracking module showing the *x*-*y* grid of scintillating fibers (left) and the front-end readout, and the Lynkeos Muon Imaging System at NNL Central Laboratory (right).

## 3. EXAMPLES OF WASTE IMAGING AND CHARACTERIZATION

### 3.1. *ILW Drums*

The development of the MIS was initially motivated by the requirement to monitor 500 L ILW drums. These drums are filled with wastes such as the metallic cladding (known as *swarf*) stripped from spent fuel elements, and then backfilled with cement. Figure 2 [1] shows a demonstration ILW drum, with a section cut away; unirradiated Magnox swarf can be seen encapsulated within the cement. Into this drum several horizontal and vertical cores were drilled. A 10×3×1 cm lead bar was placed in the top horizontal core and a cylinder of uranium, 2 cm in diameter and 3 cm long, was placed in the bottom horizontal core. The drum was imaged using the MIS at Glasgow University for a period of approximately six weeks to accumulate high statistics. Tomograms were reconstructed using an MLEM algorithm [2], and Figure 2 shows slices taken at the level of the lead and uranium. The colour scale in these tomograms (and in all subsequent tomograms in this paper) displays the value of the scattering density parameter $\lambda$, which is dependent on material radiation length.

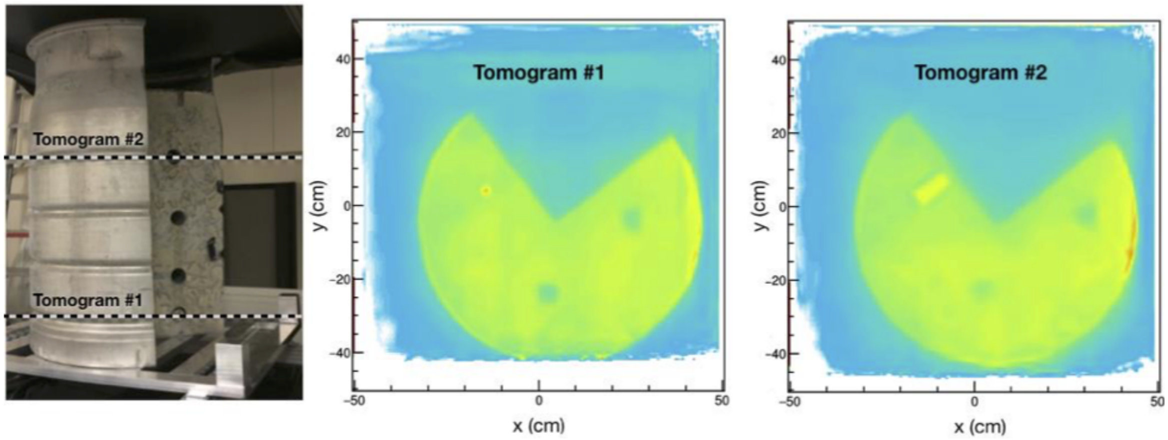

FIGURE 2: A demonstration of 500 L drum and muon scattering tomograms [1].

The tomograms show the cement-swarf matrix, the vertical cores, and the lead and uranium, clearly distinguished from each other. In the *z*-plane, the resolution of the reconstructed object positions and extents is smeared out to 1 cm accuracy. This is caused by the limited angular distribution of reconstructed muon tracks, the small magnitude of the muon scattering angle, and the subsequent difficulty in reconstructing the nearly parallel incoming and outgoing vectors. However, in the *x*-*y* plane, this resolution is at the mm level; these tomograms demonstrate that muon scattering tomography is a good candidate for nuclear waste characterization, and in the following two sections, we discuss its application to further waste forms encountered on the Sellafield site.

### *3.2. Vitrified Wastes*

The use of vitrification processes has been used in the UK for some time to reduce the volume of high-level waste and immobilize it in glass matrices. NNL has been trialling a vitrification process known as GeoMelt [3] that may be suitable for similar treatment of a wide range of intermediate-level wastes (ILW). GeoMelt vitrification destroys organic wastes and immobilizes radionuclides and heavy metals, such as those found within conventional ILW, in a stable glass waste form.

In order to evaluate the efficacy of the process, the muon imaging system at the Central Laboratory was used to inspect a variety of vitrified test products produced by NNL. The principle goal of these inspections was to determine if the waste products were homogeneously dispersed throughout the melt. An example of one such melt included a steel "top hat" container filled with grout and uranium pennies (Figure 3(a)). Muon track data were collected for a period of two weeks, with the resulting tomogram shown in Figure 3(b).

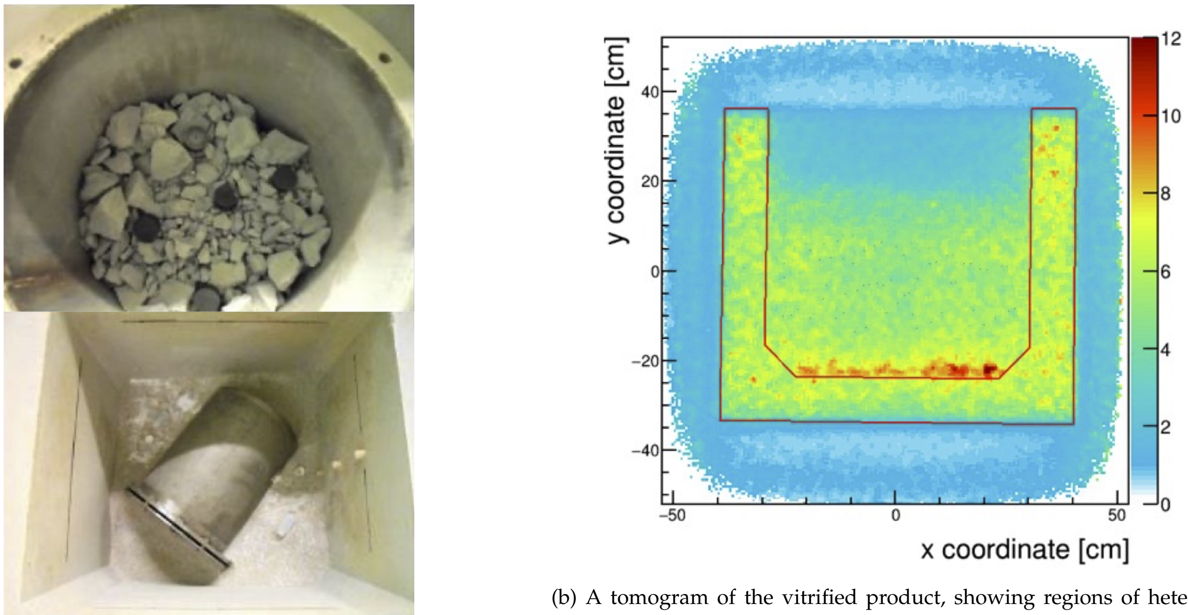

(a) The steel top hat with grout and uranium pennies inside

(b) A tomogram of the vitrified product, showing regions of heterogeneous material on the base of the container

FIGURE 3: Muography of a GeoMelt vitrified waste product.

In this image, a low-density layer can clearly be seen at the base of the crucible with localized high-Z deposits. The low-$Z$ deposit is consistent with partial melting of the steel can and the high-$Z$ inclusions are consistent with the uranium pennies. The rest of the product is homogeneous, and the height of the glass monolith can be clearly identified.

### *3.3. Corroded Sludge*

The Magnox Swarf Storage Silo (MSSS) is a facility at Sellafield used to store intermediate-level waste, principally composed of cladding stripped from spent Magnox fuel elements sent for reprocessing. The building has 22 compartments used to store the cladding as well as miscellaneous wastes from various plants on the Sellafield site. Water was used to cover the contents to eliminate the risk of pyrophoric uranium compounds being exposed to air, and this has resulted in the corrosion of the wastes. In the earliest used compartments, this results in a sludge of magnesium hydroxide and hydrogen.

The MSSS is a priority for decommissioning, and as part of this process, the waste from the compartments will be retrieved and placed inside stainless steel skips [4] and topped up with cover water to keep the waste in a wetted condition. These skips will then be placed inside a larger, concrete-lined skip known as a $3\,\mathrm{m}^3$ box (see Figure 4). These boxes will then be placed in interim storage for a period of 50 to 75 years, before being sent for final disposal in a geological disposal facility (GDF).

In order to assure UK regulators that the waste is behaving as expected during its interim storage and is safe for disposal at a future GDF, Sellafield will undertake a campaign of periodic monitoring of the boxes and their contents. This campaign, referred to as Condition Monitoring and Inspection (CM&I), will consider various parameters to infer or directly measure waste behaviour. Sellafield, working with NNL and Lynkeos Technology Ltd., is currently evaluating if muon tomography is suitable to measure the following parameters:

(i) Heterogeneous material distribution.

(ii) Inner skip integrity.

(iii) Waste height.

(iv) Water fill level.

As part of this evaluation, a scaled-down version of a 3 m$^3$ box was constructed and imaged in the MIS at Central Laboratory. The key features of the box, shown in Figure 5, are an inner skip separated into two vertical layers; the bottom layer containing six jerry cans, each filled with simulant sludge (of varying densities) to different heights; a top layer representing heterogeneous wastes and including tungsten cylinders, test pieces of unirradiated Magnox swarf, and a large steel bolt; and a concrete liner between the inner and outer skips; a 1 cm deformation along the 55 cm length of one wall of the inner skip. The skips are made of 6 mm thick stainless steel and fitted with lids of 8 mm thick steel.

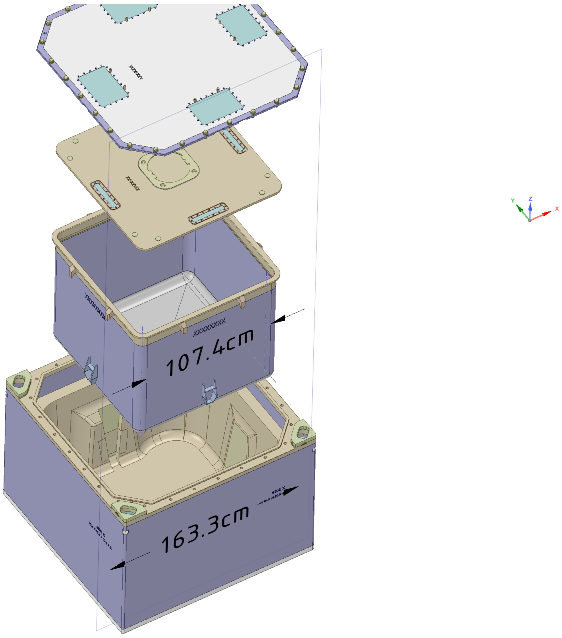

FIGURE 4: A rendering of a 3 m$^3$ box, showing the inner stainless steel skip where MSSS waste will be deposited and the outer steel box with concrete lining.

FIGURE 5: A small-scale version of a 3 m$^3$ box showing the top layer (left) of heterogeneous wastes and (right) the bottom layer with six jerry cans of simulant corroded sludge and the top layer. Also visible is the concrete liner and the 1 cm deformation of the left-hand wall of the inner skip.

Tomograms resulting from the imaging run of four weeks are shown in Figure 6. In both images, the inner and outer steel skips and the concrete liner are clearly discernible. The deformation in the inner skip wall is visible by the eye, but further analysis allows a more precise reconstruction. Figure 7 shows the position of the peak scattering values among voxels in the region of the walls for the straight wall and the deformed wall. The error bars represent the width of a Gaussian distribution fitted to the spread

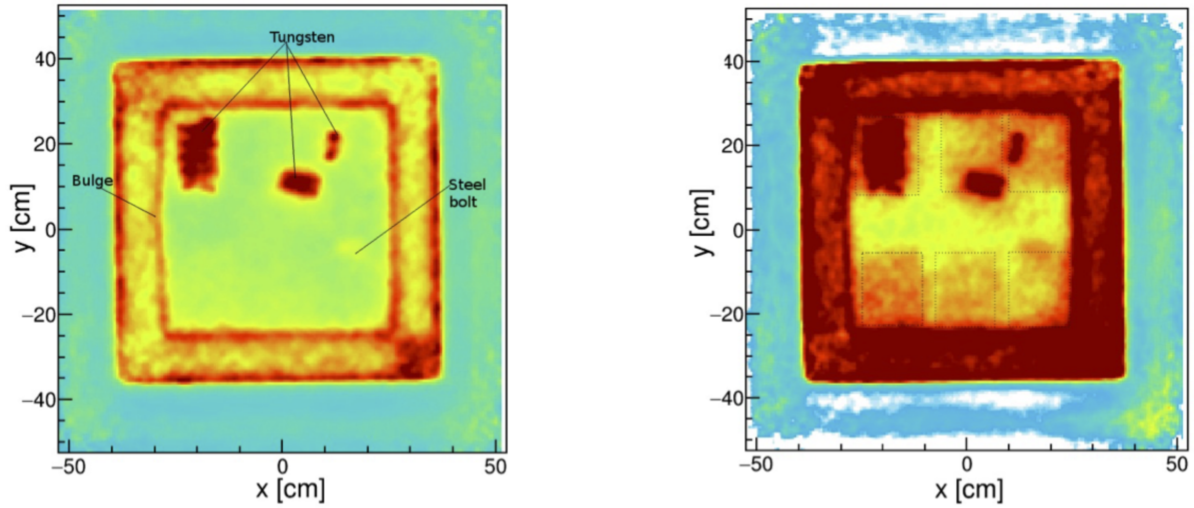

(a) An image slice taken from the top level of the inner skip

(b) An image slice taken from the bottom level of the inner skip

FIGURE 6: Tomograms of the small-scale 3 $m^3$ box.

of scattering values in the $x$ direction at each $y$ ordinate to determine the peak value and position, and the pink bands denote the nominal wall position. The location and magnitude of the deformation are correctly reconstructed. The taper in the $\lambda$ values towards 20 cm for the straight wall is caused by the box being loaded into the MIS at a slight angle with respect to the tracking modules.

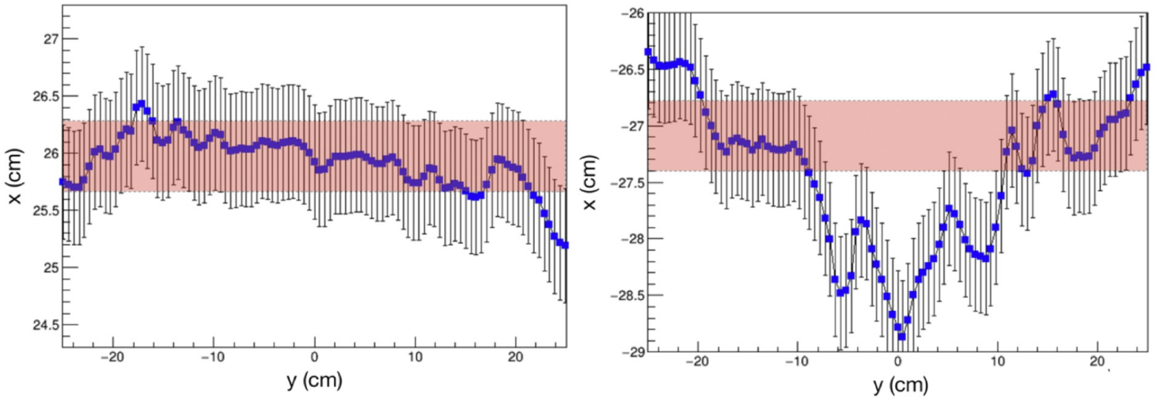

FIGURE 7: The reconstructed position of peak scattering density values for the straight wall of the inner skip (left) and the deformed wall (right). The pink bands denote the nominal wall positions.

In the top layer (Figure 6(a)), the tungsten pieces are clearly visible as was the steel bolt. It was not possible to see the swarf material. The tomogram of the bottom layer (Figure 6(b)) shows the individual containers of sludge and variations in scattering values corresponding to the different heights.

It was not possible to determine the sludge heights with a good degree of accuracy because of the “smearing” of reconstructed images in the z-plane (described in Section 3.1), and indeed, this smearing is evident in Figure 6(b) as the tungsten in the top layer can still be seen in this tomogram. To eliminate this smearing effect, one must either rotate the object of interest or use muons travelling at near-horizontal angles to the zenith. Waste plant operators are reluctant to make too many unnecessary or complicated movements of nuclear waste packages, and in the case of sludges, rotation onto a side would be impossible anyway, so the large-angle flux must be used. We currently do not have detectors configured to perform horizontal measurements, so GEANT4 simulations were performed. The simulation geometry considered a detector construction similar to that described in Section 2, but with 160 cm long fibers and tracking modules arranged horizontally. A sample of muons corresponding to two weeks of data-taking was transported through the simulation, and the same reconstruction algorithms used in experimental work were applied to the data.

Figure 8 shows the results for sludges of three different densities (2.0 $g\,cm^{-3}$, 1.67 $g\,cm^{-3}$, and 1.5 $g\,cm^{-3}$), each with a height of 50 cm and covered by 35 cm of water. The scattering density $\lambda$ is plotted against skip height, and two regions can be distinguished, corresponding to the two different materials. With knowledge of the container, inner dimensions and the average reconstructed $\lambda$ of the two materials, the position of the material boundaries can be estimated from the analysis of the slope between the two regions. In this case, the thickness of each material can be measured with 1 cm accuracy. The results also show that the measurement is independent of the sludge density: the expected linear relationship between the scattering density and material density is found, as shown in the inset plot in Figure 8.

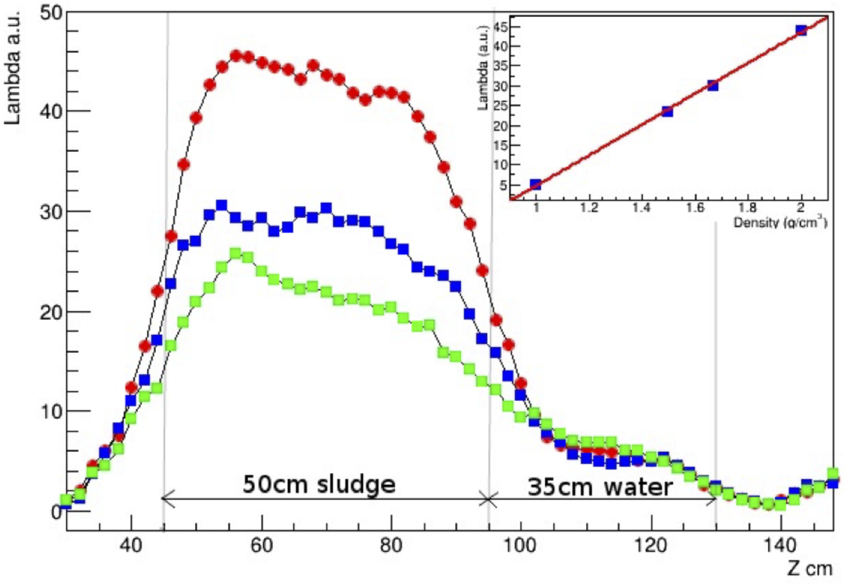

FIGURE 8: Results from simulation studies of the ability of muon tomography to measure material boundary positions. The three different curves correspond to different densities of sludge: red curve, $\rho = 2.0\,\mathrm{g\,cm^{-3}}$; blue curve, $\rho = 1.67\,\mathrm{g\,cm^{-3}}$; and green curve, $\rho = 1.5\,\mathrm{g\,cm^{-3}}$.

.

## 4. NUCLEAR SITE DEPLOYMENT

Safety is the principle and overriding concern for all operations taking place on nuclear-licensed sites. As such, it is not quite such a simple matter to install muon tracking detectors at a site like Sellafield. Before the detectors can be shipped, they must be shown to be safe for operation. The most effective method to demonstrate this is to have the detector assessed by a notified body against the relevant EU harmonized technical standards, and it is this route we followed for the deployment of the MIS at NNL central laboratory.

As part of the work assessing muon tomography for MSSS waste package monitoring for Sellafield (described in Section 3.3), we are considering the concept design of an imaging system suitable for $3\,\mathrm{m}^3$ boxes and which could be deployed at the Box Encapsulation Plant (BEP); where $3\,\mathrm{m}^3$ boxes will be processed and monitored. A rendering of this system is shown in Figure 9.

The concept is based on the existing MIS scintillating fiber construction, but with horizontal detectors for waste height measurements and larger active areas ($2\,\mathrm{m}^2$ for the vertical flux detectors and $1.6\,\mathrm{m}^2$ for the horizontal flux detectors). The top tracking modules can be moved horizontally so that packages can be lowered into the system from above.

The engineering constraints at BEP pose further challenges for site deployment. Prime amongst these is the space available for detector systems. Existing areas of the plant must be used for CM&I, and Figure 10 is representative of such an area, where waste packages are lowered into the cell from above onto the shaded blue area. It can be seen that the space for the horizontal detectors is very limited. In addition, there is maze access to the cell to maintain the bulk shielding. It would not be possible to bring the $2\,\mathrm{m}^2$ modules through this entrance, so the design must consider a modular construction of each tracking detector, such that a full detector can be constructed from submodules within the cell.

In addition to the space constraints, the radiation environment in the presence of a waste package must be considered. The $3\,\mathrm{m}^3$ boxes are not intended to provide significant shielding to protect plant personnel, and access to areas containing packages is prohibited. The gamma emission energy spectra from MSSS wastes are dominated by Cs$^{1}$37 and Co$^{6}$0, and at the distance at which detectors would be placed, gamma fluxes are in the region of $1 \times 10^{7}\,\mathrm{cm^{-2}\,s^{-1}}$. This gamma background exceeds the expected muon flux by several orders of magnitude. The detector response and methods of suppressing the background are currently being studied.

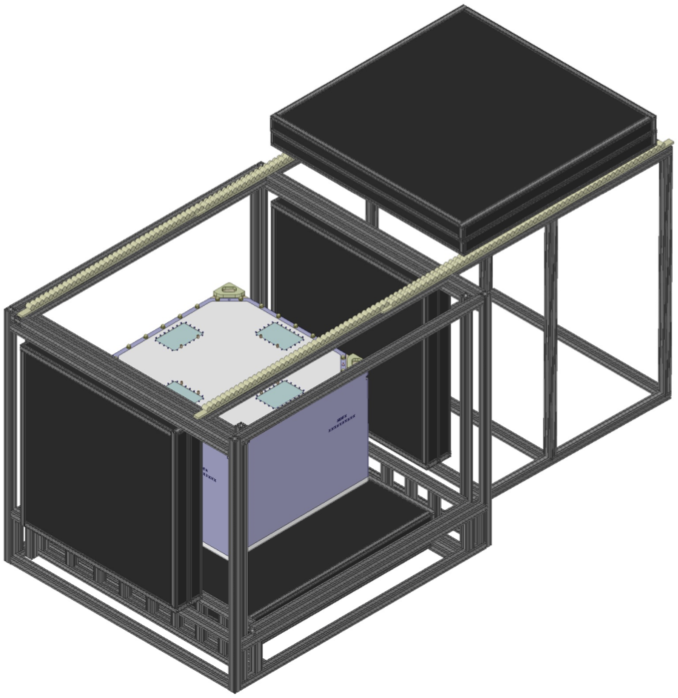

FIGURE 9: Concept design for a muon imaging system for CM&I of MSSS 3 $\text{m}^3$ boxes.

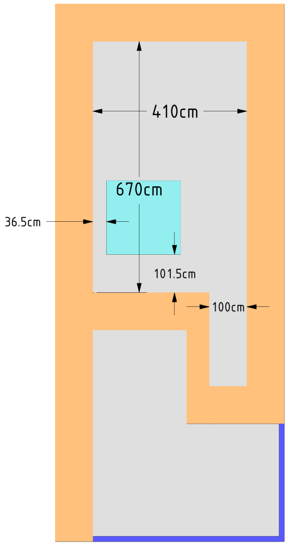

FIGURE 10: Plan of a representative cell for waste package CM&I at BEP. The blue shaded area shows the path of a waste package lowered into the cell from above.

## 5. SUMMARY

Over the last decade, the collaboration between Lynkeos Technology and NNL has made considerable progress in developing muon imaging for the passive imaging and characterization of nuclear waste. In this paper, we have presented selected examples of diverse waste forms that we have imaged during this period. The results show that muography can be considered a useful method in the toolkit of non-destructive techniques required for the safe processing and storage of wastes arising from nuclear site operations.

Deployment of muon tracking detectors at nuclear-licensed sites is laden with challenges, some of which have been discussed in this paper. However, advances in detector design, readout electronics, and fabrication methods are helping to address these challenges.

## CONFLICTS OF INTEREST

The authors declare that there are no conflicts of interest regarding the publication of this paper.

## References

[1] Mahon et al., "First-of-a-kind muography for nuclear waste characterization," Philosophical transactions of the Royal Society of London Series A **377** (2019).

[2] Yang et al., "Novel muon imaging techniques," Philosophical transactions of the Royal Society of London Series A **377** (2019).

[3] World Nuclear News, 25th July 2016,"Inauguration of GeoMelt system at Sellafield," `https://www.world-nuclear-news.org/Articles/Inauguration-of-GeoMelt-system-at-Sellafield`

[4] Nuclear Decommissioning Authority, "Packaging of Wastes from the Magnox Swarf Storage Silos at the Silos Direct Encapsulation Plant (Interim stage)," Summary of Assessment Report (2008).